International Journal of Automotive Technology, Vol. 7, No. 4, pp. 459–468 (2006)

1229–9138/2006/028–09

DYNAMIC SIMULATION MODEL OF A HYBRID POWERTRAIN AND CONTROLLER USING CO-SIMULATION – PART I: POWERTRAIN MODELLING

B. CHO* and N. D. VAUGHAN

School of Engineering, Cranfield University, Cranfield, Bedfordshire, MK43 0AL, UK

(Received 22 December 2005; Revised 20 March 2006)

ABSTRACT–The objective of this paper is the development of the forward-looking dynamic simulation model of a hybrid electric vehicle (HEV) for a fuel economy study. The specification of the vehicle is determined based on two factors, engine peak power to curb weight ratio and specific engine power. The steady state efficiency models of the powertrain components are explained in detail. These include a spark ignition direct injection (SIDI) engine, an integrated starter alternator (ISA), and an infinitely variable transmission (IVT). The paper describes the integration of these models into a forward facing dynamic simulation diagram using the AMESim environment. Appropriate vehicle and driver models have been added and described. The controller was designed in Simulink and was combined with the physical powertrain model by the co-simulation interface. Finally, the simulation results of the HEV are compared with those of a baseline vehicle in order to demonstrate the fuel economy potential. Results for the vehicle speed error and the fuel economy over standard driving cycles are illustrated.

KEY WORDS : Hybrid electric vehicle, Spark ignition direct injection, Integrated starter alternator, Infinitely variable transmission, Co-simulation

NOMENCLATURE

R_{TX} : transmission ratio
$T_{TX,in}$: transmission input torque
$T_{TX,loss}$: equivalent transmission loss torque
$T_{TX,out}$: transmission output torque
$\overline{T}_{TX,out}$: normalised transmission output torque
$\omega_{TX,in}$: transmission input speed
$\omega_{TX,out}$: transmission output speed

1. INTRODUCTION

The environmental impact of automobiles is increasingly one of the most important social issues, emphasised by the implementation of the Kyoto Protocol. To meet the required target to reduce carbon dioxides, many kinds of new technologies in the transportation sector have been suggested to improve the fuel economy and the efficiency. As a result, alternative clean vehicle technologies such as electric vehicles, hybrid electric vehicles (HEVs), and fuel cell vehicles have been suggested. However, considering the technical and infrastructural limitations, the HEV is currently seen as a ready-to-use solution.

*Corresponding author. e-mail: harry.b.cho@gmail.com

Theoretically, there is a wide variety of hybrid powertrain configurations, but they can be classified as a series, a parallel, or a power split according to the power mixing structure. The series hybrid with an ideal power source such as a diesel engine, a gas turbine or a fuel cell has great fuel saving potential, but the cost and the technical challenge are obstacles at this moment. Consequently, the parallel mild hybrid with an integrated starter alternator (ISA) like Honda Insight (DOE, 2001a) and the power split hybrid using two electric machines (EMs) such as Toyota Prius (DOE, 2001b) are the only commercially available variants.

In the parallel mild HEV, the ISA is connected to the engine crankshaft and can be used as a motor to assist the engine or as a generator to charge the battery. Therefore, there are many complex compromises in the interactions between mechanical design and control algorithms, since they involve several energy storage and power transfer components. However, this configuration can minimise the additional cost of hybridization and the reengineering effort of the conventional powertrain.

The objective of this paper is the development of the forward-facing dynamic simulation model of a HEV for the fuel economy study. The specification of the vehicle is determined based on two factors, engine peak power to

curb weight ratio and specific engine power. The steady state efficiency models of the powertrain components are explained in detail followed by the integration into a dynamic simulation diagram in AMESim environment. The controller designed in Simulink is combined with the physical powertrain model by the co-simulation interface. The simulation results of the HEV are compared with those of a baseline vehicle.

2. VEHICLE CONFIGURATION

2.1. Reference Vehicles

There are quite many HEVs are in mass production or scheduled in next few years. shows a broad spectrum of the HEVs from a 2-seater passenger car to full size pickup trucks in North American market (EPA, 2005b). Although the HEVs have many applications, midsize cars and sport utility vehicles (SUVs) are the majority of them. In this study, a SUV is chosen as a target vehicle segment because it is more effective to hybridise a SUV rather than a passenger car because of relatively poor efficiency, low extra cost, and easy packaging.

Table 1. HEVs in north american market (EPA, 2005b).

Model	Vehicle type	Hybrid type
In mass production		
Chevrolet Silverado	Pickup Truck	ISA
Ford Escape	SUV	Power Split
GMC Sierra	Pickup Truck	ISA
Honda Accord	Midsize Car	ISA
Honda Civic	Compact Car	ISA
Honda Insight	2 Seater	ISA
Lexus RX 400h	SUV	Power Split
Mazda Tribute	SUV	Power Split
Mercury Mariner	SUV	Power Split
Toyota Highlander	SUV	Power Split
Toyota Prius	Midsize Car	Power Split
Year 2006		
Lexus GS 450h	Midsize Car	Power Split
Nissan Altima	Midsize Car	Power Split
Saturn VUE	SUV	ISA
Toyota Camry	Midsize Car	Power Split
Year 2007		
Chevrolet Equinox	SUV	ISA
Chevrolet Malibu	Midsize Car	ISA
Chevrolet Tahoe	SUV	Power Split
GMC Yukon	SUV	Power Split
Year 2008		
Chevrolet Silverado	Pickup Truck	Power Split
Ford Fusion	Midsize Car	Power Split
GMC Sierra	Pickup Truck	Power Split
Mercury Milan	Midsize Car	Power Split

7 of the 9 SUVs in are compact SUVs based on the passenger car platforms. These vehicles listed in Table 2. Specification of reference SUVs (CarsDirect, 2005; Car and Driver, 2005). are selected as the reference vehicles with a large engine if there are multiple options. As shown in the table, the average fuel economy is 8.3 and 10.8km/L in the city and the highway cycle respectively. These values are relatively lower than those of the passenger cars that are equipped with similar size engines because of the heavy weight, wide tires, large frontal area, and high aerodynamic drag.

2.2. Engine Size

Two comparative studies of hybrid powertrains (Husted, 2003; Walters *et al.*, 2001) show the strong relationship between the vehicle curb weight and the engine power and size. This approach can give a general guideline to determine the proper engine size for a vehicle weight. However, the vehicles considered in these studies are only a few HEVs, so the result is based on the limited number of vehicles in different segments and hybridization ratios. Applying this methodology to SUVs, which

Table 2. Specification of reference SUVs (CarsDirect, 2005; Car and Driver, 2005).

Model	Engine		Weight [kg]		Fuel economy [km/L]	
	Size [L]	Power [kW]	Curb	Gross	City	High way
Equinox	3.4	138	1660	2300	8.1	10.6
Escape	3.0	149	1496	1987	8.5	10.6
RX 330	3.3	178	1751	2424	8.1	10.6
Tribute	3.0	149	1507	1987	8.5	10.6
Mariner	3.0	149	1510	2041	8.5	10.6
VUE	3.5	186	1578	2220	8.5	11.9
High-lander	3.3	172	1656	2431	8.1	10.6
Average	3.2	160	1594	2199	8.3	10.8

generally have heavy weight and large engines than passenger cars, more data of the SUVs should be gathered and analysed.

It is not easy to classify a vehicle as a SUV because there is no unique and clear definition. In this study, 2005 model year SUVs on the fuel economy guide (EPA, 2005a) are considered. The engine size, peak power and curb weight of 76 SUV models with 107 engine variants are listed in Appendix. To remove the exceptional cases, those powered by diesel, natural gas, and turbocharged engines are removed. If there are more than one driveline options, a 2-wheel drive (2WD) automatic transmission (AT) or continuously variable transmission (CVT) model was selected instead of a 4-wheel drive (4WD) or manual transmission.

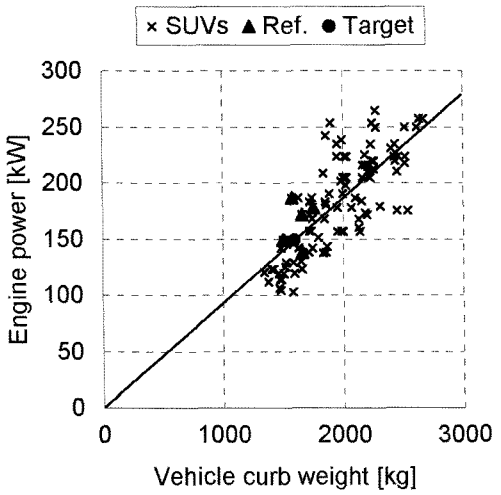

Figure 1. Relationship between vehicle curb weight and engine peak power.

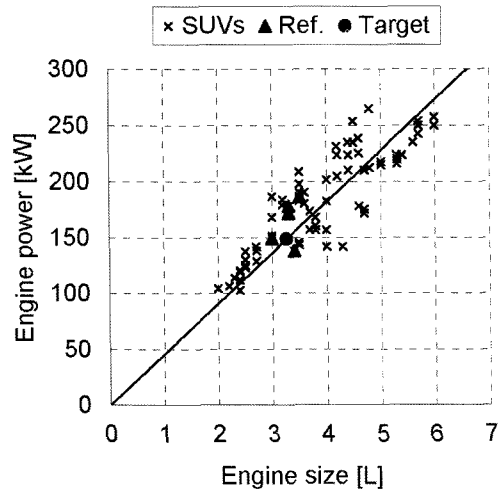

Figure 2. Relationship between engine peak power and engine size.

Figure 1 depicts the engine peak power to vehicle curb weight ratio. The curb weight is distributed from 1345 kg to 2670 kg, and the peak engine power is from 103 kW to 265 kW. The trend line gives an average value of 93.2 kW/1000 kg. It is clear that the reference vehicles are positioned in low power and weight area. The average curb weight of these is 1594 kg shown in Figure 2, and when the trend line is applied, the required engine power is 149 kW. This is 7% lower than 160 kW, which is the average of the 7 reference vehicles because most of them have additional small engine options.

To estimate the proper engine size, the specific engine power should be examined. From Figure 2, the average specific engine power for the SUVs is 45.4 kW/L. As a result, the engine size required to output 149 kW is 3.3 L. It is well matched with the average value of 7 reference vehicle engines which is 3.2 L.

2.3. Type of Powertrain

Additional important factors of the hybrid powertrain are types of the engine and the transmission. A recent study (Husted, 2003) shows that most of the HEVs use advanced gasoline engines and CVTs. A spark ignition direct injection (SIDI) engine with a CVT is selected as a base powertrain because it is one of the best combinations of the gasoline engine based vehicles.

A stratified charge SIDI engine has good efficiency in low power region frequently used in normal driving conditions. In addition, its low friction loss can reduce the cranking time from the idle stop and maximise the energy absorbed by the regenerative braking in HEVs. CVTs has been considered as an ideal transmission type but suffering from the driveability issues because it tends to operate the engine on the most efficient point which is generally located in high torque and low speed. If it is combined with SIDI engine, it is possible to operate the engine in relatively low torque and overcome this drawback.

Most of the CVTs adopt a metal push belt or a chain as a torque transfer device but are limited using under 3L engine applications. One of the high power solutions is a infinitely variable transmission (IVT), a power split full toroidal CVT with geared neutral function as illustrated in Figure 3. IVT have been developed by Torotrak during last few decades. The geared neutral function implemented by an epicyclic gear set, a shunt gear, and a chain can omit the torque converter which is the most inefficient part of the conventional AT or CVT, and applicable up to full size SUVs (Brockbank and Heumann, 2002). Additionally, according to the shunt gear ratios, IVT can get a ratio from reverse to high overdrive.

2.4. Hybridization

The final step of the powertrain configuration for the

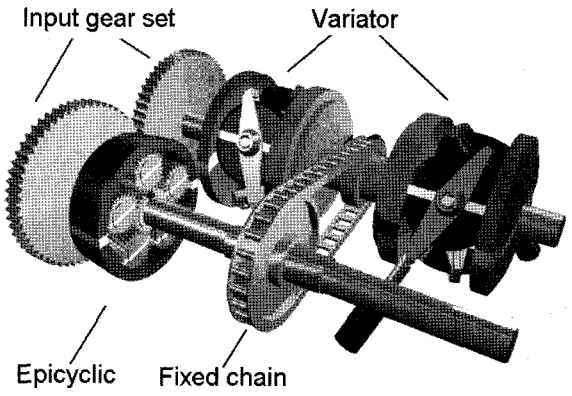

Figure 3. Schematic diagram of IVT (Torotrak, 2005).

HEV is the hybridisation. Although Honda Insight is the first mass production HEV of this type, it is a purpose-built 2-seater car with an exceptional styling aluminium body and narrow low rolling resistance tyres. On the contrary, Civic and Accord have their hybrid versions based on the conventional vehicles (Ogawa *et al.*, 2003; Hanada, 2005). The power and torque capacity of the ISA are obtained from the scaling of these HEVs. Honda mentions that the maximum power of the ISA used in Accord, 12 kW, is increased from that of Civic, 10 kW, according to the vehicle weight increment from 1200 kg to 1600 kg (Kabasawa and Takahashi, 2005). Using the same scaling factor, 15 kW ISA is selected for the baseline vehicle with 2200 kg gross weight. The battery size is another critical factor of the cost, the space and the weight of the HEV. There are little obvious guideline, but because Honda uses same battery capacity from Insight to Accord it is also adopted for this study and is reviewed as part of the exercise.

2.5. Vehicle Specification

The specification of the vehicles is summarized in Table

Table 3. Specification of vehicles.

	Baseline	HEV
Engine	3.3 L SIDI	←
Transmission	IVT	←
ISAD	–	15 kW
Battery	–	6.0 Ah/144 V
Mechanical accessory	1kw	–
Electric accessory	–	1 kW
GVWR	2200 kg	2220 kg
Tyre size	235/70 R16	←
Frontal area	2.7 m^2	←
Drag coefficient	0.38	←

3. The weight of the battery is added to the HEV, and the mechanical accessory of the engine is converted to the electric load to the battery in the case of the HEV. Other parameters are set as the average values of the reference vehicles.

3. STEADY STATE POWERTRAIN MODEL

3.1. Engine

A few SIDI engines have been commercialised but it is hard to find a 3.3 L stratified charge SIDI engine and access the experimental data of the fuel consumption. To generate the brake specific fuel consumption (BSFC) map of the engine, the algorithm suggested by Horn *et al.* (2002; Shayler *et al.*, 1999; Shayler *et al.*, 2001a; Shayler *et al.*, 2001b) is adopted for this study. Considering the NOx problem, the simulation limits the stratified charge operation under 3200 rpm and 5 bar brake mean effective pressure (BMEP) and it is assumed that The exhaust gas recirculation (EGR) mechanism is involved in stratified charge mode operation. Outside of this region, the engine works in the homogeneous charge without EGR.

Figure 4 shows the result of BSFC map. The minimum BSFC is 265 g/kWh that is equivalent to 31% efficiency and a typical value of this size of the gasoline engines. The iso-BSFC lines have discontinuities at the changing points of the operation mode between the stratified and the homogeneous charge operation. Within the low power region the BSFC is quite better than typical multi point injection (MPI) engine and this is the beneficial effect of the SIDI engine. The maximum BMEP shown as a thick line is less than 10 bar, which is lower than typical value because the rich fuel injection to increase the output torque at high throttle is not considered. The rich fuelling by the modified injection and spark timing is difficult to be predicted in this sort of model. It may

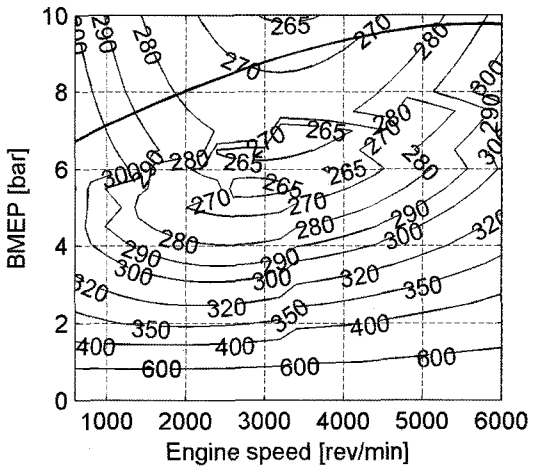

Figure 4. BSFC map of the 3.3L SIDI engine.

affect to the vehicle performances such as the top speed and the maximum acceleration but there is little effect to examine the fuel economy study in standard driving cycles.

3.2. Integrated Starter Alternator and Battery

The basic specification of the EM can be defined with maximum torque, power, and speed. They depend on the applied technology and the dimensions, but there is no general rule to predict the specific performance. In particular, the crankshaft installed ISA should have a short axial length because of the limited space between the engine and the transmission. There is no mass production ISA with 15 kW power, so it is the best way to refer the ISA of Accord which has 12/14 kW maximum power for motoring/generating and +/−136 Nm maximum torque (Kabasawa and Takahashi, 2005). Applying the scaling factor of 1.25, the maximum power and torque are 15/17.5 kW and +/−170 Nm.

Predicting the efficiency of the ISA is more difficult because there is no experimental data of the ISAs except for that of Insight in ADVISOR (NREL, 2002). However, Honda's researches show the improvement of the efficiency from Insight to Civic (Ogawa *et al.*, 2003) and the comparison between Civic and Accord (Kabasawa and Takahashi, 2005). According to these studies, the power loss of the ISA used in Accord is around 30% less than that of Insight. Figure 5 shows the resulting efficiency map considering this improvement. In most commonly used region, the efficiency is over 90% and it is quite well matched with the efficiency map of Accord.

The battery model is also a carry-over from the Insight. As like the ISA, the battery also has been improved from insight to Accord significantly. The main improvement is the reduction of the internal resistance by the modification of the current collector (Yusaku and Kosaka,

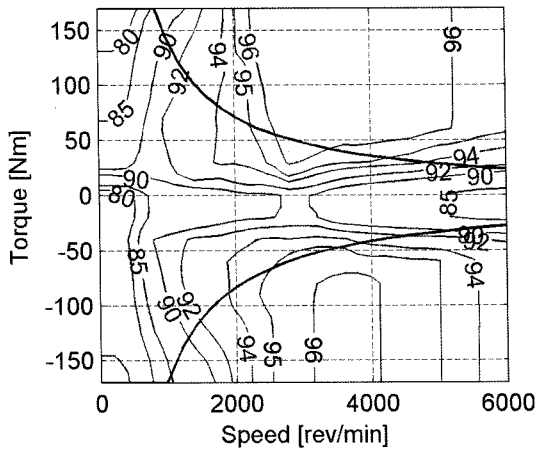

Figure 5. Efficiency of the ISA including the power electronics loss.

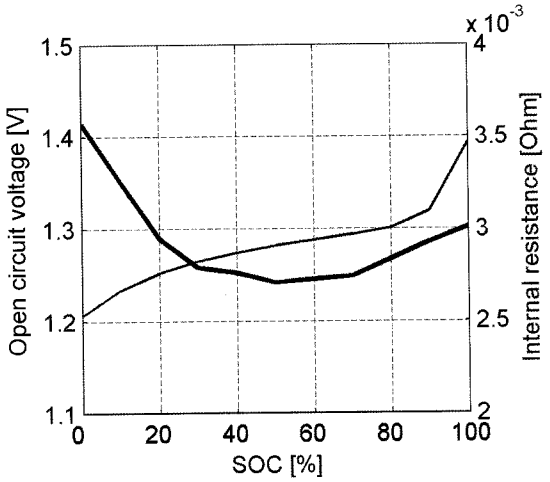

Figure 6. OCV and internal resistance of the battery.

2005). To account for this, the internal resistance of the battery is modelled with 30% reduced value from the data of the Insight in ADVISOR. The open circuit voltage (OCV) and the internal resistance to the state of charge (SOC) are shown as a thin and a thick line respectively in Figure 6.

3.3. Transmission

The basic specification of the IVT used in this study is summarized in Table 4. The detailed dynamics of the IVT is quite complex due to the torque transfer mechanism of the toroidal variator (Fuchs *et al.*, 2002; Hasuda and Fuchs, 2002). An additional difficulty to model the IVT is the control of the variator because the pressure on the pistons of the rollers in the full toroidal variator makes the torque at the input and the output side. Consequently, the speed ratio cannot be controlled directly from the pressure and the quite complex calculation is needed to match the torques in both side to obtain the desired speed ratio (Burke *et al.*, 2003).

To avoid these complexities and develop the time efficient simulation program, it is modelled as an ideal CVT with loss torque at the input side. According to the research from Torotrak, the loss torque is mainly depends on the torque and the transmission ratio, but the effect of the speed is relatively small. To describe this characteristic simply, a pre-calculated map of the loss torque at the

Table 4. Specification of IVT.

Item	Value
Overdrive ratio	0.287
Final drive ratio	5.20
Final drive efficiency	98.0%

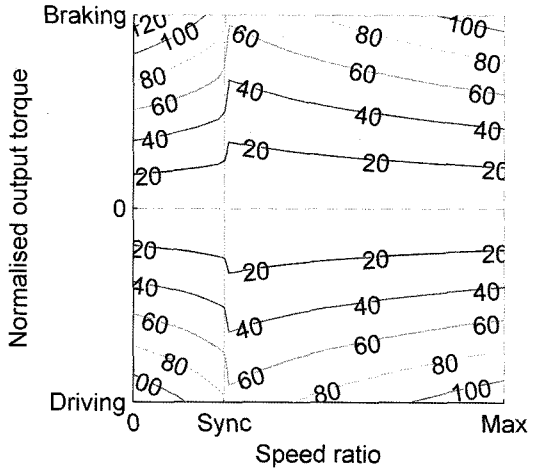

Figure 7. Torque loss of IVT.

input side including the torque to drive the oil pumps is generated as a function of output torque and the transmission ratio. These relationships can be expressed as below.

$$\omega_{TX,out}=R_{TX}\omega_{TX,in} \tag{1}$$

$$T_{TX,in}-T_{TX,loss}=R_{TX}T_{TX,out} \tag{2}$$

The loss torque tends to be proportional to the output torque normalised by the maximum value at the given speed ratio. To increase the accuracy of the loss torque calculation in the simulation, the grid of the loss torque map is based on the ratio and the normalised output torque.

Table 5. Dynamic parameters.

Inertia [kg m^2]		Time constant [sec]	
Engine	0.165	Engine throttle	0.10
Flywheel	0.100	ISA torque	0.05
ISA	0.100	IVT ratio	0.10
IVT input	0.200	IVT clutch	0.20
IVT output	0.100	Brake	0.05
One wheel	0.500	Battery voltage	0.10

$$T_{TX,loss}=T_{TX,loss}(R_{TX},\bar{T}_{TX,out}) \tag{3}$$

$$\bar{T}_{TX,out}\equiv\frac{T_{TX,out}}{\max(T_{TX,out}(R_{TX}))} \tag{4}$$

Figure 7 shows the result of the calculation. The loss torque is increased as the output torque towards maximum. It is mainly caused by the power loss of the oil pumps. The change of the loss along the speed ratio is not very significant. The efficiency is the best around the synchronization ratio because the drag loss by the relative speed difference between the components is lowest.

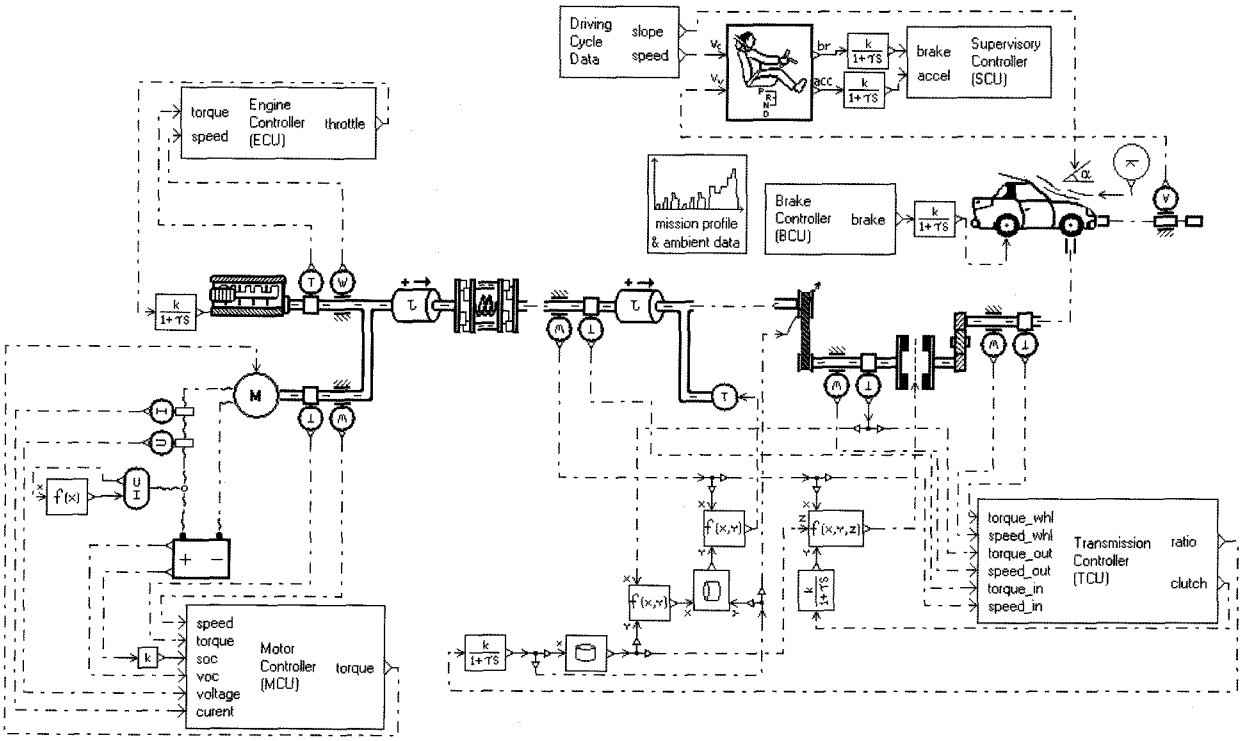

Figure 8. Dynamic simulation diagram of the HEV.

4. DYNAMIC SIMULATION

4.1. Integration of Powertrain Model

For the dynamic simulation of the powertrain, AMESim (Imagine, 2004) is used as a programming tool. It offers intuitive and convenient physical modelling environment and a large number of pre-built libraries for the vehicle powertrain components. Figure 8 illustrates the forward-facing simulation model of the HEV implemented in AMESim. All the controllers that appear as simple black boxes are Simulink co-simulation interfaces, which communicate data with the control algorithm implemented in Simulink during the simulation. The lumped rotating inertia is considered at the engine output and the transmission input side, and that of the transmission output side is included in the vehicle model. The dynamics of all actuators including the throttle, the transmission ratio and the clutch, the brake, and the battery voltage are modelled as first order dynamics. The parameters related to the dynamics used in the simulation are listed in Table 5.

4.2. Co-simulation with Controller

There are more than one power sources and sinks in parallel HEVs. The engine and the EM can propel the vehicle with the fuel and the electric energy in the battery, and the EM and the brake can reduce the vehicle speed by absorbing the kinetic energy. To harmonise these sources and sinks effectively, an additional controller, supervisory controller, is positioned on the logically higher level of the local controllers and responsible to organise them.

This study adopts a supervisory control strategy for the mild hybrid powertrain with a CVT, which is proposed and detailed in Part II of this paper (Cho and Vaughan, Submitted). This control strategy operates the CVT powertrain optimally from the viewpoint of the tank-to-wheel efficiency and distributes the torque between the engine and the EM to maximise the engine efficiency and maintain the battery SOC within an appropriate level.

The top-level simulation diagram of the controllers is illustrated in Figure 9. The vehicle modelled in AMESim outputs all sensor signals to the supervisory control unit (SCU). The supervisory controller calculate the required control values including the engine torque, the ratio of the transmission, the engagement of the transmission clutch, and the brake torque. The local controllers translate the required physical values to the real control signal according to the scaling and the saturation of the actuators. Only the engine control unit (ECU) and the motor control unit (MCU) among the local controllers receives the sensor signals directly because the idle control function requires the engine speed.

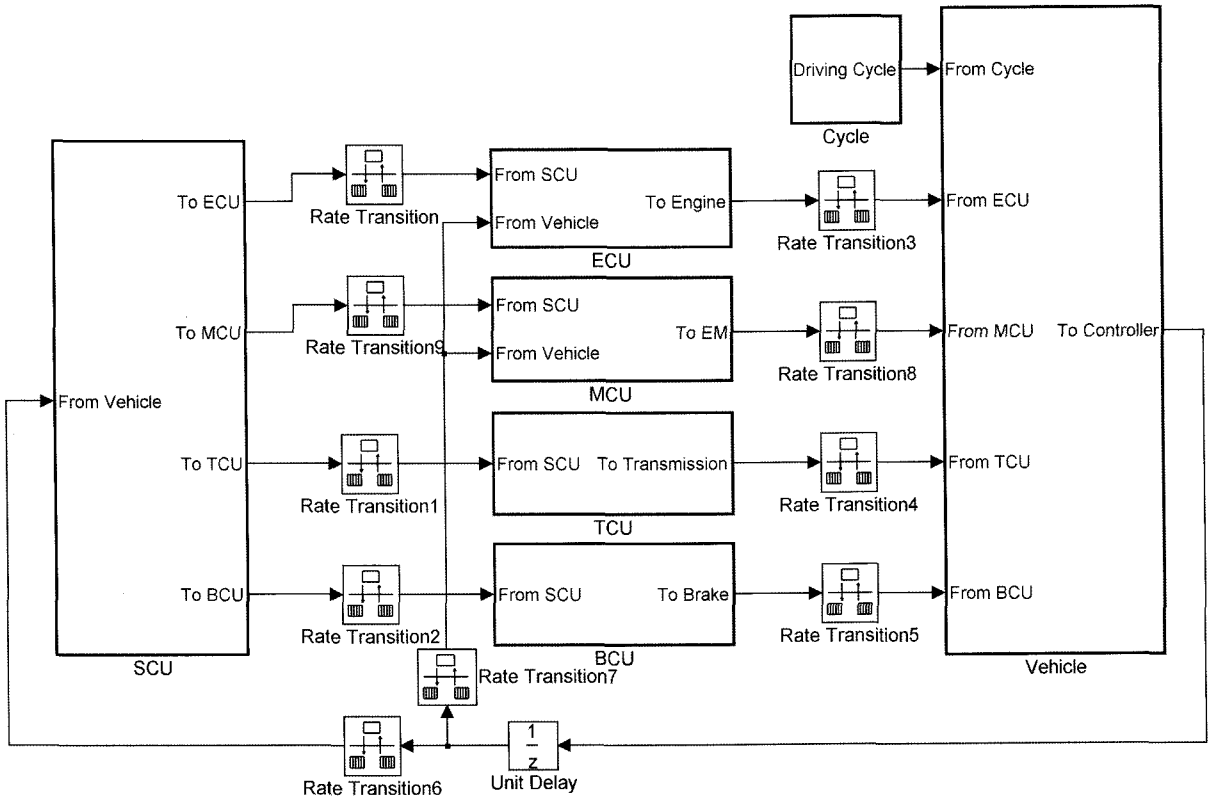

Figure 9. Top-level diagram of the simulation in simulink.

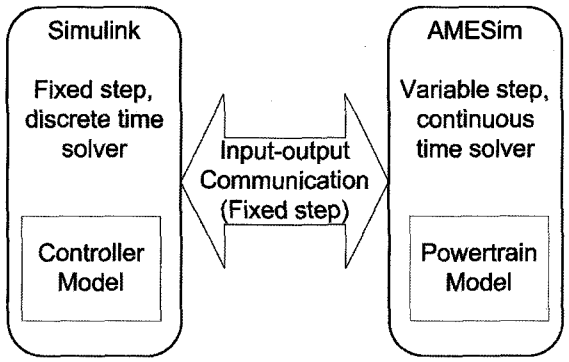

Figure 10. Working principle of AMESim-Simulink co-simulation interface.

Each controller has independent control loop time. The ECU, the MCU, and the brake control unit (BCU) is calculate the command signal at 1 kHz, and the transmission control unit (TCU) is running on 8 msec time base. The timer of the SCU is set to the slowest local controller, so 8 ms is also applied. To match the different running rate among the controllers and the vehicle, several rate transition blocks are inserted between them. The reference vehicle speed of driving cycles is supplied from the separate block.

Even though AMESim offers a convenient way to model physical systems, it is not more efficient than Simulink (Mathworks, 2005) to implement the logical algorithms generally required to design the controller. To combine the benefits from both of the software, AMESim offers co-simulation interface with Simulink. depicts the working principle of the co-simulation interface. The vehicle modelled in AMESim has continuous states and the default variable step solver is used. The controller model has only discrete states and the minimum loop time is 1ms, so the fixed time discrete solver is used for the simulation. Generally, the continuous states requires shorter time step than the controller. In the co-simulation, the two solvers communicate at the fixed interval and the powertrain model in AMESim is shown as a simple algebraic block in Simulink. Therefore, the simulation time can be reduced by avoiding the redundant calculation of the control algorithm.

5. SIMULATION RESULTS

5.1. Vehicle Speed Error

The forward facing simulation of the powertrain needs a driver model. In this work, the standard driver model in AMESim is adopted. This model consists of two PID controllers, which are related to the accelerator and the brake pedal control. The PID gains should be tuned to maintain the vehicle speed error within given bounds.

Table 6. Gains of the driver model.

Gains	Accelerator	Brake
Proportional	0.20	0.20
Integral	0.02	0.02
Differential	0.35	0.15

Table 7. Vehicle speed error.

Vehicle	cycles	allowable tolerance* [km/h]	speed error [km/h]	
			rms	peak
Baseline	nedc	2.0	0.21	1.77
	ftp-75	3.2	0.35	2.32
	hwfet	3.2	0.49	1.92
	10-15		0.19	1.00
HEV	nedc	2.0	0.20	1.80
	ftp-75	3.2	0.33	1.97
	hwfet	3.2	0.49	1.84
	10-15		0.17	0.90

*(EPA, 1975; EC, 2004)

From the default values, the gains have been tuned intuitively and the results are in Table 6. The same values are applied to both the baseline and HEV because the change of the driver gains can affect the fuel consumption even though it is a little. The differential gain of the brake is smaller than that of the accelerator because the vehicle speed tends to be slow down by the aerodynamic drag and the rolling resistance without any forces.

The speed error in the simulation over the driving cycles are summarised in Table 7. For the synthetic cycles such as New European Driving Cycle (NEDC) and Japanese 10–15, the error is relatively small. On Federal Test Procedure –75 (FTP-75) and Highway Fuel Economy Test (HWFET) which are real world and dynamic driving schedules the error is larger but the peak values are in the allowable tolerances. Therefore, it can be concluded that the driver gains are tuned properly.

5.2. Variation of SOC

The SOC variation over the driving cycle is summarized in . The starting SOC level is set same as the target SOC, 60%, for all driving cycles. The lowest point is 52% in HWFET cycle, and the highest value is 65% in FTP-75. Generally, the appropriate limit of the SOC change is +/–10%. Therefore, the result of the SOC change is within a reasonable boundary, so the selected battery capacity is suitable for this size of mild hybrid application. In addition, the final SOC after the operation of the driving cycles is slightly higher than the initial values in FTP-75 mode. In HWFET, the final SOC is just 1%

Table 8. SOC variation.

	SOC [%]			
	NEDC	FTP-75	HWFET	10-15
Initial	60	60	60	60
Max.	53	65	60	58
Min.	63	58	52	63
Final	62	64	59	62

Table 9. Fuel economy of baseline vehicle and HEV.

Vehicle	Fuel economy [km/L] (Improvement [%])			
	NEDC	FTP-75	HWFET	10-15
Baseline	10.0	9.8	12.6	9.1
HEV	11.4 (14.0)	11.4 (16.3)	12.9 (2.4)	11.3 (24.2)

below the initial SOC. Therefore, it is clear that fuel economy improvement of the HEV does not depend on the battery energy consumption.

5.3. Fuel Economy

The comparison of the overall fuel consumption over the standard driving cycles is most important because the fuel economy improvement is the main target of the hybrid vehicles. Table 9 shows the comparison of the fuel economy between the baseline and the HEV. The HEV shows considerable improvement from the baseline vehicle. In 10–15 mode the improvement is 24.2%, and 2.4% in HWFET which is the worst case. These differences are based on the characteristics of the driving cycles. 10–15 mode has relatively long idle time and low average speed. On the other hand, HWFET has little idling and high average speed. The mild hybrid can get most of the advantages from the idle stop and frequent regenerative braking. Therefore, it is hard to get a significant improvement in HWFET cycle. In NEDC and FTP-75, the improvement is 14.0% and 16.3% respectively, and these values are at least more than expected levels in the recent studies of the mild hybridized SUV(MacBain, 2002; Simopoulos *et al.*, 2001).

6. CONCLUSIONS

The conclusions of this study are the following.

(1) A compact SUV was configured as a target vehicle for the hybridization. A 3.3L SIDI engine and a CVT were selected through the analysis of the weight to power ratio and the engine specific power. The hybridised version was equipped with a 15kW ISA and a 6Ah, 144V battery.

(2) The steady state efficiency model of the hybrid powertrain was derived from the computer simulation and the existing data with the appropriate scaling.

(3) The dynamic simulation model is developed in AMESim-Simulink co-simulation environment. This method offers the convenient modelling of the physical system and the efficient simulation using the simultaneous running of the two solvers.

(4) The fuel economy improvement of the hybrid SUV ranges from 2.4 to 24.2% and is considered particularly advantageous in the urban driving cycles.

ACKNOWLEDGEMENT–Acknowledgments to Torotrak Development Ltd for use of a simulation package and data of the IVT, and Imagine SA for the simulation software AMESim and technical support.

REFERENCES

Brockbank, C. and Heumann, H. (2002). Delivery of IVT for a 5 liter SUV: addressing the concerns of geared neutral. *Innovative Fahrzeun-Getriebe.*, Bad Mergentheim, Germany

Burke, M., Briffet, G., Fuller, J., Heumann, H. and Newall, J. (2003). Powertrain efficiency optimization of the torotrak infinitely variable transmission (IVT). *SAE 2003 World Congress.* Detroit, Michigan, USA, *SAE Paper No.* 2003-01-0971.

Car and Driver. (2005). *Capsule Review.* Car and Driver. website, cited 14 Jan. 2005, available from http://www.caranddriver.com.

CarsDirect (2005). *New Cars: Specs & Features.* CarsDirect. website, cited 9 Nov. 2005, available from http://www.carsdirect.com.

Cho, B. and Vaughan, N. D. (Submitted). Dynamic Simulation Model of a Hybrid Powertrain and Controller using Co-simulation - Part II : Control strategy. *Int. J. Automotive Technology.*

DOE (2001a). *U. S. Department of Energy technology snapshot - Featuring the Honda Insight.* In Energy, D. O. (Ed.), Argonne National Laboratory.

DOE (2001b). *U. S. Department of Energy technology snapshot - Featuring the Toyota Prius.* In Energy, D. O. (Ed.), Argonne National Laboratory.

EC (2004) *Council Directive 70/220/EEC : Measures to be Taken against Air Pollution by Emissions from Motor Vehicles.* Office for Official Publications of the European Communities.

EPA (1975). *CFR Part 600 : Fuel Economy Regulations for 1977 and Later Model Year Automobiles.* US Environmental Protection Agency.

EPA (2005a). *Model Year 2005 Fuel Economy Guide.* IN AGENCY, U. S. E. P. (Ed.), NREL.

EPA (2005b). *New Hybrid Vehicles Increase Gas-Saving Options for Consumers.* U.S. Environmental Protection Agency.

Fuchs, R. D., Hasuda, Y. and James, I. B. (2002). Full toroidal IVT variator dynamics. *SAE 2002 World Congress.* Detroit, Michigan, USA, *SAE Paper No.* 2002-01-0586.

Hanada, K., Masaaki, K., Ishikawa, S., Imai, T., Matsuoka, H. and Adachi, H. (2005). Development of a hybrid system for the V6 midsize sedan. *SAE World Congress.* Detroit, Michigan, USA, *SAE Paper No.* 2005-01-0274.

Hasuda, Y. and Fuchs, R. (2002). Development of IVT variator dynamic model. *Koyo Engineering J. English Edn.*, 24–28.

Horn, G. (2002). *The Prediction of Fuel Economy and Pollutant Emissions to Assess the Benefits of Direct Injection Gasoline Engines.* Ph. D. Dissertation. University of Nottingham. Nottingham. UK.

Husted, H. L. (2003). A comparative study of the production applications of hybrid electric powertrains. *Future Transportation Technology Conf.,* Costa Mesa, California, USA.

Imagine (2004). *AMESim.* 4.2.0 Edn., Roanne, France.

Kabasawa, A. and Takahashi, K. (2005). Development of the IMA motor for the V6 hybrid midsize sedan. *SAE World Congress.* Detroit, Michigan, USA, *SAE Paper No.* 2005-01-0276.

Macbain, J. A. (2002). Simulation influence in the design process of mild hybrid vehicles. *SAE 2002 World Congress.* Detroit, Michigan, USA, *SAE Paper No.* 2002-01-1196.

Mathworks (2005). *Simulink.* 6.2 Edn. The Mathworks Inc., Natick, Massachusetts, USA.

NREL (2002). *Advisor 2002 Edn.* Golden, Colorado, USA, National Renewable Energy Laboratory.

Ogawa, H., Matsuki, M. and Eguchi, T. (2003). Development of a power train for the hybrid automobile-The civic hybrid. *SAE 2003 World Congress.* Detroit, Michigan, USA, *SAE Paper No.* 2003-01-0083.

Shayler, P. J., Horn, G. and Eade, D. (1999). Predictions of fuel economy for types of DISI and MPI spark ignition engines. *Int. Conf. Integrated Powertrain Systems for a Better Environment.* Birmingham, UK, 149–163.

Shayler, P. J., Jones, S. T., Horn, G. and Eade, D. (2001a). Characterisation of DISI emissions and fuel economy in homogeneous and stratified charge modes of operation. *SAE Int. Fall Fuels and Lubricants Meeting and Exhibition.* San Antonio, Texas, USA, *SAE Paper No.* 2001-01-3671.

Shayler, P. J., Jones, S. T., Horn, G. and Eade, D. (2001b). DISI engine spark and fuel injection timings. Effects, compromise and robustness. *SAE Int. Fall Fuels and Lubricants Meeting and Exhibition.* San Antonio, Texas, USA, *SAE Paper No.* 2001-01-3672.

Simopoulos, G. N., Macbain, J. A., Schneider, E. D. and Wingeier, E. W. (2001). Fuel economy improvements in an SUV equipped with an integrated starter generator. *SAE Int. Truck and Bus Meeting and Exposition.* Chicago, Illinois, USA, *SAE Paper No.* 2001-01-2825.

Torotrak (2005). *How It Works?.* Torotrak Development Ltd., website, cited 5 May 2005, available from http://www.torotrak.com.

Walters, J., Husted, H. and Rajashekara, K. (2001). Comparative study of hybrid powertrain strategies. *SAE Future Transportation Technology Conf. and Exposition.* Costa Mesa, California, USA, *SAE Paper No.* 2001-01-2501.

Yusaku, N. and Kosaka, H. (2005). Development of the intelligent power unit for the V6 hybrid midsize Sedan. *SAE World Congress.* Detroit, Michigan, USA, *SAE Paper No.* 2005-01-0275.